Research article

Journal of Human, Health and Halal Metrics; 2020, 1(2): 15-23
https://doi.org/10.30502/JHHHM.2020.210209.1005

Biodegradable brush copolymer nanomicelles for smart release of doxorubicin

Aliyeh Ghamkhari[1*], Nazila Taghavi[2]

1- *Institute of Polymeric Materials, Faculty of Polymer Engineering, Sahand University of Technology, Tabriz, Iran.*
2- *Department of Chemistry, Payame Noor University, Tehran, Iran.*

Submission: 2 December 2019 ***Revision***: 23 June 2020 ***Acceptance***: 12 July 2020

Abstract

Background and objective: In cancer therapy, smart and biocompatible nanocarriers are the most important features of therapeutic agents. pH-sensitive drug delivery nanocarriers which can be remotely prompted are attractive for patients management and therapeutic purposes. In this paper, a novel nanocarrier was fabricated and investigated for controlled release of Doxorubicin (DOX).

Materials and methods: Self-assembled nanomicelles containing a hydrophilic core and a hydrophobic shell were successfully prepared using poly(2-hydroxyethyl methacrylate-graft-ε-caprolactone)-block-poly (methacrylic acid) [P(HEMA-g-CL)-*b*-(PMAAc)] brush copolymer by combining reversible addition-fragmentation chain transfer polymerization (RAFT) and ring open polymerization (ROP). Morphology, micelles properties, and pH-sensitive behavior were studied by field emission scanning electron microscopy (FESEM), transmission electron microscope (TEM) and distribution laser-scattering (DLS) analysis.

Results and conclusion: Molecular weight of P(HEMA-g-CL) and [P(HEMA-g-CL)-*b*-PMAAc] samples was obtained as 15117 g mol^{-1} and 25887 g mol^{-1}, respectively. The polydispersity index (PDI) of P(HEMA-g-CL) (PDI = 1.14) and [P(HEMA-g-CL)-*b*-PMAAc] (PDI = 1.19) synthesized by RAFT polymerization were relatively low, suggesting good control of the technique over the process. The self-assembled micelles were pH-sensitive and showed low critical concentration in water. TEM showed that the micelles had nanosized spherical shape with average size of 35 nm. The critical micelle concentration (CMC) value of [P(HEMA-g-CL)-*b*-PMAAc] micelle was 0.025 g l^{-1}. Encapsulation efficacy of the nanomicelle was 94.3%. Release behavior of DOX from the nanomicelles revealed that rate of core release could be efficiently controlled by body temperature and pH. In this regard, the release rate at pH of 7.4 and 5.4 was 54.73% and 36.52%, respectively. As a conclusion, structure of the nanocarrier and its controllable characteristics introduced it as appropriate vehicle in drug delivery.

Keywords: Cancer therapy, Doxorubicin, Nanomicelle, pH-sensitive

1. Introduction

Recently, progress in nanotechnology has been significant due to its potential in disease prevention, treatment, and diagnosis [1]. Drug delivery approaches have been developed progressively in transfer of therapeutic medicines to target tissues

* Correspondence to: Aliyeh Ghamkhari; e-mail: aliyeh_ghamkhari@yahoo.com

with low toxicity and high efficiency [2-5]. Anti-cancer drugs pose adverse impacts on healthy tissues in the way of target organs via blood circulation. Targeted delivery of medicines have been introduced to administer the cytotoxic drugs specifically in target cancer cells [6-7].

Nano-sized self-assembled polymeric micelles prepared from amphiphilic copolymers are popular because of their applications in gene and drug delivery [8-10]. They have several advantages including water solubility improvement of drugs, decreasing their side effects, prolonging their circulation time, improving their bioavailability, and passive targeting of them in tumor tissues by enhanced permeability and retention effect [11-13].

Amphiphilic graft copolymers have been developed from hydrophobic biodegradable polymers grafted to synthetic or natural polymers [14]. Amphiphilic copolymers such as poly (2-hydroxyethylmethacrylate) grafted to aliphatic polyesters such as poly(ε-caprolactone) (PCL), poly(lactide) (PLA), and poly(lactide-co-glycolide) (PLGA) are of the most evaluated chemicals as a result of their desirable biocompatibility and *in vivo* biodegradability [15-17].

There are few reports about hydrophobic polymers grafted to hydrophilic polymers because of the difficulties in the synthesis process. Grafted copolymer micelles have several advantages such as enhanced stability, optimized length and density of the graft affecting drug loading, and optimal tumor targeting owing to the high density of targeting ligands prepared by hydrophilic grafting per macromolecule [18-20].

Composition, size of particles and morphology of carriers can be optimized through the synthesis process. Various copolymers are available for controlled/living radical polymerization techniques [21,22]. These include nitroxide-mediated polymerization (NMP) [23], atom transfer radical polymerization (ATRP) [24], reversible addition fragmentation chain transfer (RAFT) [25,26], and ring open polymerization (ROP) [27]. RAFT polymerization is a powerful method for synthesis of amphiphilic block copolymers with predefined composition, well-defined structure, and narrow dispersity [28]. Synthesis by a wide range of various monomers such as 2-hydroxy-ethyl-methacrylate (HEMA) [29], acrylic acid (AA) [30], and N-isopropylacrylamide (NIPAm) [31], which can be inserted into the chain transfer agent (CTA), are feasible by this method.

At this work, we used a simple way to fabricate polymeric nanomicelles for targeted cancer therapy. Fabrication, characterization, and self-assembly behavior of novel pH-sensitive co-polymer of poly(2-hydroxyethyl methacrylate-graft-ε-caprolactone-block-poly (methacrylic acid) [P(HEMA-g-CL)-*b*-(PMAAc)] was investigated. At first, the copolymer of poly(2-hydroxyethyl methacrylate-graft-ε-caprolactone [P(HEMA-g-CL)] were synthesized via ROP and RAFT methods. Then, MAAc was success-fully synthesized using RAFT polymerization. Doxorubicin (DOX) was inserted into the nanomicelles by ionic interaction and hydrogen bonding.

2. Materials and methods

2.1. Materials

RAFT agent (4-cyano-4-[(phenylcarbothioyl) sulfanyl] pentanoic acid) was synthesized in our laboratory [25]. Chemicals of HEMA, methacrylic acid, $Sn(Oct)_2$, and ε-caprolactone (ε-CL) were purchased from Merck (Germany) and azobisisobutyronitrile (AIBN) from Fluka (Switzerland). DOX was prepared from Zhejiang (China). Dimethyl sulfoxide (DMSO) and other reagents were obtained from Merck (Germany).

2.2. Fabrication of poly(2-hydroxyethyl methacrylate-graft-ε-caprolactone) P(HEMA-g-CL) copolymers

Reaction was done by glove-box approaches under N_2 atmosphere. In this regard, RAFT agent (20 mg, 0.07 mmol) and AIBN (3.0 mg, 0.01 mmol) were transferred to flask and stirred for 1 h. Then, ε-CL (4.40 g, 38.55 mmol), HEMA (0.5

g, 3.84 mmol), $Sn(Oct)_2$ (0.4 g, 1.97 mmol), and toluene (3 ml) were added to the flask and the mixture was heated to 110 °C for 3 h. The reaction was stopped by declining the temperature in ice. The P(HEMA-g-CL) copolymer was precipitated in ether. At the end, the precipitate was dried under vacuum at ambient temperature for 24 h (Scheme 1a).

2.3. Fabrication of poly(2-hydroxyethyl methacrylate-graft-ε-caprolactone)-block-metaacrylic acid copolymer [P(HEMA-g-CL)-*b*-PMAAc]

Block copolymerization was done by using P(HEMA-g-CL) as macro-RAFT agent and MAAc monomer. A flask was charged with P(HEMA-g-CL) (1 g, 0.06 mmol), MAAc monomer (1 g, 11.6 mmol), AIBN (3 mg, 0.01 mmol), and dimethylformamid (10 ml). The mixture was degassed and moved to oil bath at 85 °C for 48 h. Then, the [P(HEMA-g-CL)-*b*-MAAc)] copolymer was precipitated in diethyl ether. According to the last step, the precipitate was dried under vacuum at ambient temperature for 24 h (Scheme 1b).

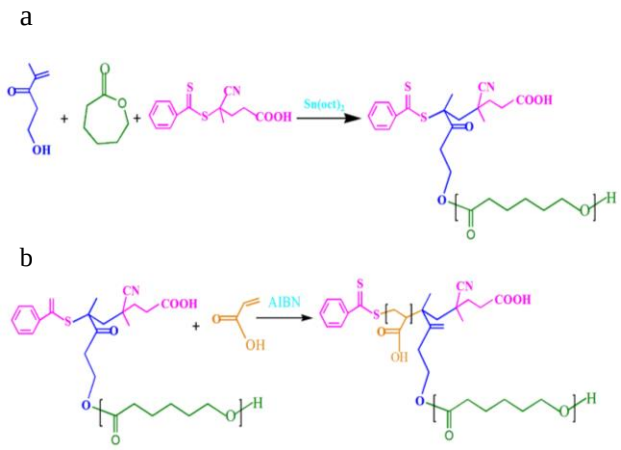

Scheme 1- Fabrication of a) poly(2-hydroxyethyl methacrylate-graft-ε-caprolactone) P(HEMA-g-CL); b) poly(2-hydroxyethylmethacrylate-graft-ε-caprolactone)-block-poly(methacrylic acid) [P(HEMA-g-CL)-*b*-PMAAc]

2.4. Preparation of DOX-[P(HEMA-g-CL)-*b*-PMAAc] nanomicelles

100 mg [P(HEMA-g-CL)-*b*-PMAAc] in 2 ml deionized water and DOX (10 mg) were mixed in a 25-ml vial and stored at 25 ºC for 48 h in darkness. Finally, DOX-[P(HEMA-g-CL)-*b*-PMAAc] was poured into a dialysis bag. The dialysis bag was directly immersed in 500 ml of distilled water. After 48 h, water was refreshed to remove DMSO solvent.

2.5. Characterization of [P(HEMA-g-CL)-*b*-PMAAc] and DOX-[P(HEMA-g-CL)-*b*-PMAAc] nanomicelles (Scheme 2)

Size exclusion analyses was done by a Waters 1515 (USA) gel permeation chromatography (GPC) equipped with Breeze 1515 isocratic pump and 7725 manual injector.

Fourier transform infrared (FT-IR) spectra of the samples were achieved by Shimadzu apparatus (Model 8101M, Japan) within the range of 4000 to 400 cm^{-1} wavenumbers.

Proton nuclear magnetic resonance (^{1}HNMR) spectra were prepared at 25 °C by FT-NMR (400 mHz) Bruker spectrometer (Germany). The samples were prepared in deuterated DMSO.

Determination of CMC was done by preparation of pyrene stock solution (6×10^{-7} mol l^{-1}) in acetone that was stored at 5 °C for further use. To measure steady-state fluorescence spectra, the pyrene stock solution was added to deionized water to give pyrene concentration of 12×10^{-7} mol l^{-1}. Then, acetone-free pyrene solution was added followed by solutions of polymeric micelles at concentration of 0.008, 0.01, 0.04, 0.08, and 0.1 g l^{-1} at pH 3-4. Pyrene fluorescence intensity ratios (I337/I333) were plotted against logarithm of the synthesized di-block copolymer concentrations (Log C).

Size measurement of the nanocomposites was performed by laser-scattering technique (Zetasizer Nano ZS90, Malvern, UK) at 25 °C. Field emission scanning electron microscope (FESEM) (Model 1430 VP, UK) and Transmission Electron

Microscope (TEM) (Model CM10-TH, Netherland) were used for determination of nanomicelles morphology.

Encapsulation efficiency of DOX-[P(HEMA-g-CL)-*b*-PMAAc] nanoparticles was detected according to the following equation.

$$EE(\%) = \frac{\text{Mass of drug in nanomicelles}}{\text{Mass of initial added DTX}} \times 100$$

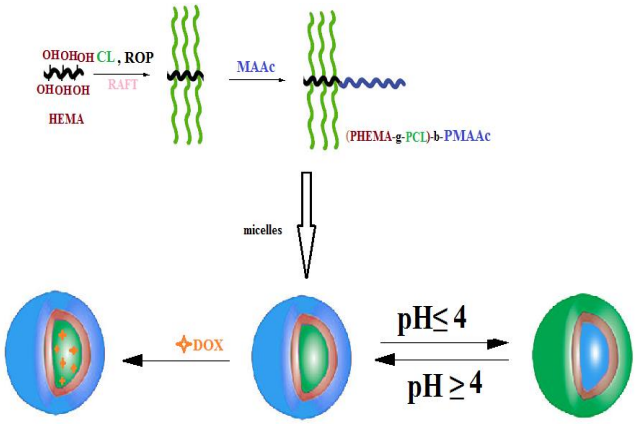

Scheme 2- Structure of pH-sensitive [P(HEMA-g-CL)-*b*-PMAAc] and DOX-loaded [P(HEMA-g-CL)-*b*-PMAAc] nanomicelles

3. Results and discussion

3.1. Characterization of [P(HEMA-g-CL)-*b*-PMAAc] copolymer

FT-IR spectra of P(HEMA-g-CL) and [P(HEMA-g-CL)-*b*-PMAAc] copolymers are shown in Figure 1. Graph of P(HEMA-g-CL) showed the transmittance bands of stretching C–O–C at 1253 cm^{-1}, stretching C–O at 1303 cm^{-1}, stretching carbonyl at 1722 cm^{-1}, stretching aliphatic C–H at 2935 cm^{-1}, and stretching O–H at 3475 cm^{-1}. Graph of [P(HEMA-g-CL)-*b*-PMAAc] showed the typical bands of both P(HEMA-g-CL) and P(MAAc). The main transmittance bands were included to stretching carbonyl at 1652 cm^{-1}, stretching aliphatic C–H and bending C–H at 2916 and 2850 cm^{-1}, and O–H at 3433 cm^{-1}.

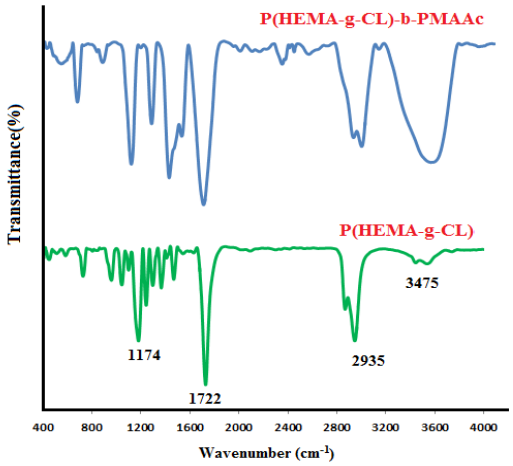

Figure 1- FTIR spectra of a) P(HEMA-g-CL), and b)[P(HEMA-g-CL)-*b*-PMAAc] copolymers

Successful fabrication of poly(HEMA-g-CL) and [P(HEMA-g-CL)-*b*-PMAAc] copolymers was confirmed by ^{1}HNMR spectroscopy. ^{1}HNMR spectra of P(HEMA-g-CL) revealed chemical shifts at 0.76−0.8 ppm (a) and 1.24−1.54 ppm (g,f,h), and 2.26 ppm (b) correlated with the methylene protons of PCL backbone and RAFT backbone, respectively. Chemical shifts at 2.8 ppm (e) and 3.3 ppm (k) were attributed to –CO-CH_2 and –CH_2-OH protons, respectively. Chemical shift at 3.9−4.2 ppm (i,c,d) was related to CH_2-O and methylene protons of PCL and PHEMA. Furthermore, the chemical shift at 7.9 ppm was related to aromatic protons of the RAFT agent (Figure 2a). As observed in the ^{1}HNMR spectra of [P(HEMA-g-CL)-*b*-PMAAc] copolymers, all the peaks were adopted with the copolymer (Figure 2b).

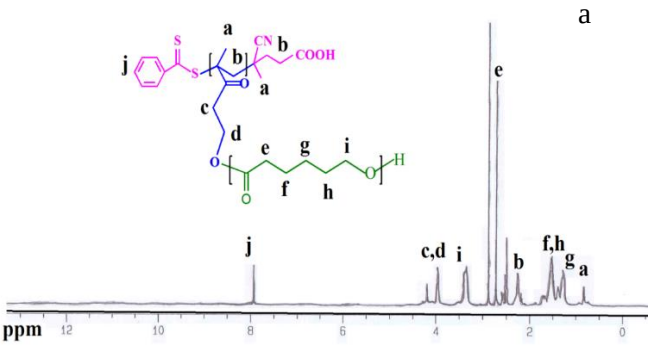

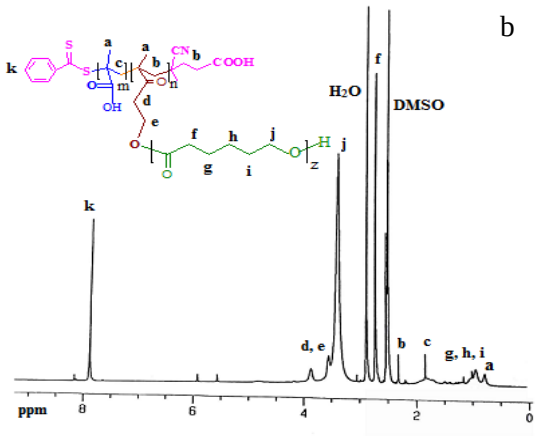

Figure 2- ^{1}HNMR spectrum of a) P(HEMA-g-CL), and b)[P(HEMA-g-CL)-*b*-PMAAc] copolymers

GPC chromatograms of P(HEMA-g-CL) and [P(HEMA-g-CL)-*b*-PMAAc] samples are presented in Figure 3. P(HEMA-g-CL) and [P(HEMA-g-CL)-*b*-PMAAc] fabricated by RAFT polymerization showed relatively low PDI of 1.14 and 1.19, respectively, which suggest an appropriate control of RAFT technique over the process. Molecular weights of the two copolymers achieved by GPC and ^{1}HNMR are compared in Table 1.

Table 1- Comparison of P(HEMA-g-CL) and [P(HEMA-g-CL)-*b*-PMAAc] characteristics achieved by GPC and ^{1}HNMR

Sample	M_n[a] (GPC)	M_n[b] (^{1}HNMR)	M_w[a]	PDI[a]
P(HEMA-g-CL)	15117	14768	17233	1.14
[P(HEMA-g-CL)-*b*-PMAAc]	25887	25345	30705	1.19

M_n: number average molecular weight; M_w: weight average molecular weight; PDI: polydispersity index

3.2. Characterization of [P(HEMA-g-CL)-*b*-PMAAc] nanomicelles

3.2.1. Morphology

Morphology of the micelles was evaluated by FESEM and TEM. Images of TEM indicates spherical shape (Figure 3a). The sphericity with approximate diameter of 35 nm is correlated with the primary micelles containing PCL as hydrophobic core and PHEMA and PMAAc blocks as a mixed hydrophilic shell. The morphology was further studied by FESEM (Figure 3b). It also indicated spherical shape and average diameter of 45 ±5 nm for the micelles. It is observed that the self-assembled nanomicelles of the brush copolymers are well dispersed individually in the medium.

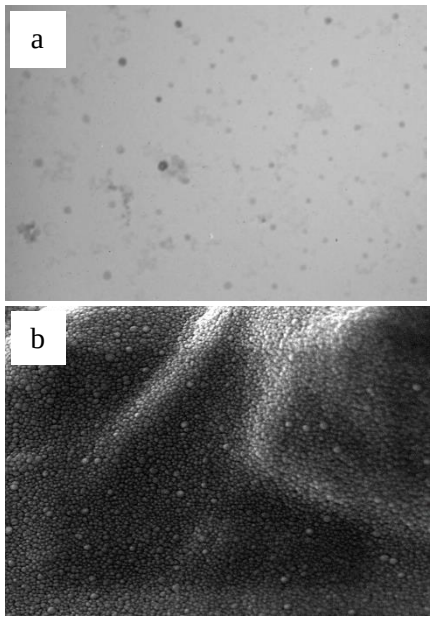

Figure 3- Images of a) TEM and b) FESEM of [P(HEMA-g-CL)-*b*-PMAAc] nanomicelles

3.2.2. Critical micelle concentration of the nanomicelles

Plot of fluorescence intensity for [P(HEMA-g-CL)-*b*-PMAAc] nanoparticles at 25 °C is depicted in Figure 4 and CMC of the nanomicelle was 0.025 g l^{-1} that is the least concentration required for nanomicelles formation.

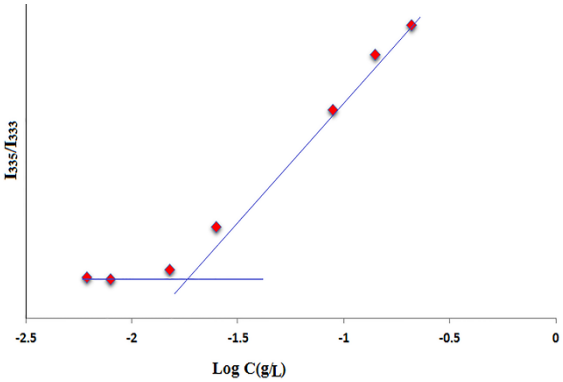

Figure 4- Fluorescence intensity of [P(HEMA-g-CL)-*b*-PMAAc] nanomicelles against logarithm of concentration

3.2.3. pH-sensitivity of [P(HEMA-g-CL)-b-PMAAc] nanomicelles

pH is an important factor when applying pH-sensitive polymers. The weak acids such as carboxylic acids are able to either release or accept proton under environmental pH changes [33]. DLS results confirmed pH sensitivity of the nanomicelles. Particle size of the brush copolymers was obtained by DLS at different pH (Figure 5). Mean particle size of the nanomicelles was 158, 279, and 124 nm at pH of 7, ≤ 4, and ≥ 9, respectively. The least size observed at pH 9, which was probably due to deprotonation of PMAAc at basic pH, leading to reduced diameters. Sizes of the particles obtained by TEM and FESEM were smaller than DLS. TEM imaging is done in the absence of solvent compared to the hydrodynamic diameter determined in a solution by DLS [25].

a

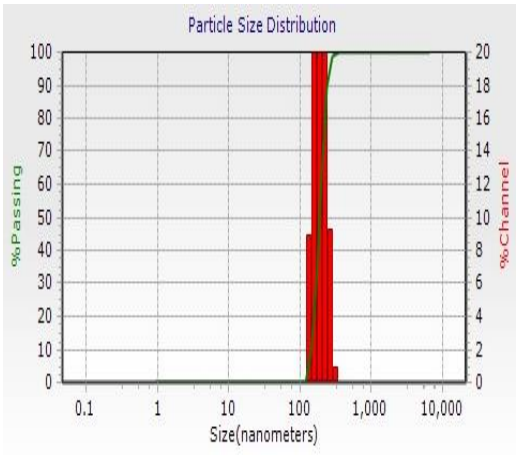

b

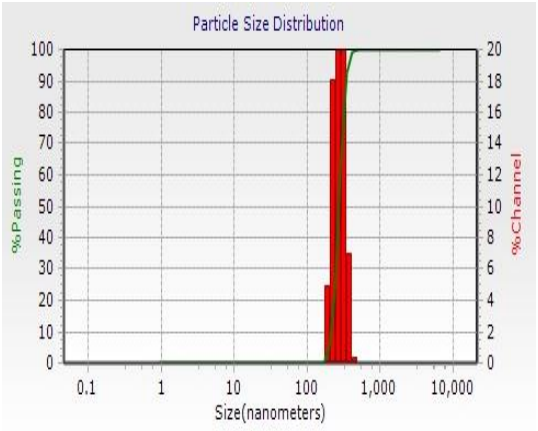

c

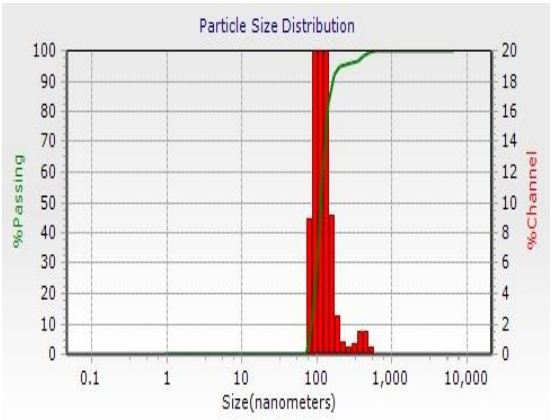

Figure 5- DLS diagrams of [P(HEMA-g-CL)-*b*-PMAAc] nanomicelles at a) pH = 7, b) pH ≤ 4, and c) pH ≥ 9

3.3. Controlled release of DOX from the nanomicelles

Encapsulation was done by a simple dialysis method. For this purpose, DOX and [P(HEMA-g-CL)-*b*-PMAAc] were dissolved in DMSO. Then, dialysis was done against distilled water. During the self-assembling process of the nanomicelles, DOX entered to the hydrophobic core (PCL). As calculated, 94.4% of the drug was loaded into [P(HEMA-g-CL)-*b*-PMAAc] nanomicelles. The drug release profile is shown in Figure 6. *In vitro* release behaviors of DOX at pH of 5.4 and 7.4 at 37 °C were examined. In this regard, the conjugated DOX was mainly released under acidic pH. A burst release was observed at pH = 5.4 after 7 h owing to protonation of PMAAc carboxyl groups that weaken the interaction between the copolymer and DOX. Then, drug release continued at slower rate so that about 55% of DOX was released at pH = 5.4 after 102.5 h. In comparison, a lower release rate was observed at pH = 7.4 because of the strong electrostatic interaction of the copolymer and DOX, thanks to deprotonation of the carboxylic groups in PMAAc copolymer and their interaction with the positively charged drug at internal space of the nanomicelles.

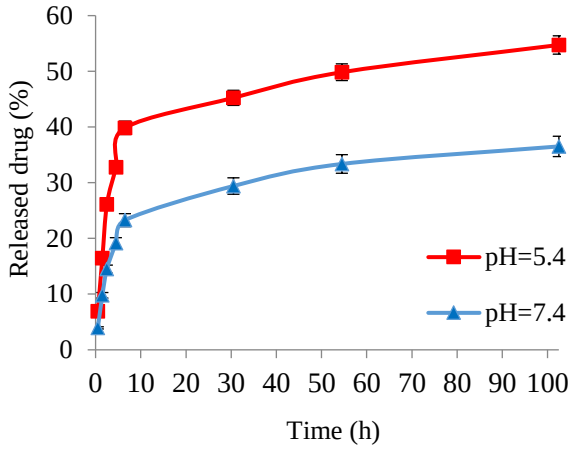

Figure 6- Release profiles of DOX from [P(HEMA-g-CL)-*b*-PMAAc] nanomicelles *in vitro*

4. Conclusions

HEMA and ε-CL were reacted by RAFT and ROP polymerization in the presence of AIBN and $Sn(oct)_2$ to synthesize PHEMA-g-PCL copolymers. Then, P(HEMA-g-CL)-*b*-PMAAc graft copolymer consisting of pH-sensitive PMAAc hydrophilic shell and biodegradable hydrophobic PCL core was fabricated by ROP and RAFT polymerization and macromonomer approach. The amphiphilic copolymers showed different behavior at different pH and were able to self-assemble into micelles in water with CMC of 0.025 g l^{-1}. According to TEM and FESEM images, size of P(HEMA-g-CL)-*b*-PMAAc micelles was in the range of 35-45 ±5 nm and they have spherical shape. The biodegradable P(HEMA-g-CL)-*b*-PMAAc nanomicelles released a higher concentration of DOX at higher rate at pH 5.4 compared to 7.4. This feature introduces the complex as a potential carrier to smartly deliver the drugs to the target organs.

5. Conflict of interest

The authors declare that they have no conflict of interest.

References

1. Valkenburg KC, de Groot AE, Pienta KJ. Targeting the tumour stroma to improve cancer therapy. Nature reviews Clinical Oncology. 2018; 15(6): 366-381. https://doi.org/10.1038/s41571-018-0007-1

2. Joshi N, Yan J, Levy S, Bhagchandani S, Slaughter KV, Sherman NE. et al. Towards an arthritis flare-responsive drug delivery system. Nature Communications. 2018; 9(1): 1275. https://doi.org/10.1038/s41467-018-03691-1

3. Rao Z, Ge H, Liu L, Zhu C, Min L, Liu M. et al. Carboxymethyl cellulose modified graphene oxide as pH-sensitive drug delivery system. International Journal of Biological Macromolecules. 2018; 107: 1184-1192. https://doi.org/10.1016/j.ijbiomac.2017.09.096

4. Patil PB, Uphade KB, Saudagar RB. A review: osmotic drug delivery system. Pharma Science Monitor. 2018; 9(2): 283-300.

5. Ding L, Li J, Wu C, Yan F, Li X, Zhang S. A self-assembled RNA-triple helix hydrogel drug delivery system targeting triple-negative breast cancer. Journal of Materials Chemistry B. 2020; 8: 3527-3533. https://doi.org/10.1039/C9TB01610D

6. Munjal M. Nanoparticles-preparation, technology, evaluation and used in targeted drug delivery system. The Pharma Innovation Journal. 2018; 7(11): 373-377.

7. Krishnakumar K. Nano sponges: a targeted drug delivery system and its applications. GSC Biological and Pharmaceutical Sciences. 2019; 7(3): 40-47. https://doi.org/10.30574/gscbps.2019.7.3.0098

8. Davaran S, Fazeli H, Ghamkhari A, Rahimi F, Molavi O, Anzabi M, Salehi R. Synthesis and characterization of novel P (HEMA-LA-MADQUAT) micelles for co-delivery of methotrexate and Chrysin in combination cancer chemotherapy. Journal of Biomaterials Science, Polymer Edition. 2018; 29(11): 1265-1286. https://doi.org/10.1080/09205063.2018.1456026

9. Massoumi B, Ghamkhari A, Agbolaghi, S. Dual stimuli-responsive poly (succinyloxy-ethylmethacrylate-b-N-isopropylacrylamide) block copolymers as nanocarriers and respective application in doxorubicin delivery. International Journal of Polymeric Materials and Polymeric Biomaterials. 2018; 67(2): 101-109. https://doi.org/10.1080/00914037.2017.1300901

10. Ghamkhari A, Massoumi B, Agbolaghi S. An *in vitro* focus on doxorubicin hydrochloride delivery of novel pH-responsive poly (2-succinyloxyethyl-methacrylate) and poly [(N-4-vinylbenzyl), N, N-

diethylamine] diblock copolymers. Polymer International. 2018; 67(3): 283-291.
https://doi.org/10.1002/pi.5504

11. Yin H, Wang H, Li Z, Shu D, Guo P. RNA micelles for the systemic delivery of anti-miRNA for cancer targeting and inhibition without ligand. ACS Nano. 2018; 13(1): 706-717.
https://doi.org/10.1021/acsnano.8b07948

12. Brandt JV, Piazza RD, dos Santos CC, Vega-Chacon J, Amantea BE, Pinto GC. et al. Synthesis and colloidal characterization of folic acid-modified PEG-b-PCL Micelles for methotrexate delivery. Colloids and Surfaces B: Biointerfaces. 2019; 177: 228-234.
https://doi.org/10.1016/j.colsurfb.2019.02.008

13. Xiong D, Zhang X, Peng S, Gu H, Zhang L. Smart pH-sensitive micelles based on redox degradable polymers as DOX/GNPs carriers for controlled drug release and CT imaging. Colloids and Surfaces B: Biointerfaces. 2018; 163: 29-40.
https://doi.org/10.1016/j.colsurfb.2017.12.008

14. Chen F, Li Y, Fu Y, Hou Y, Chen Y, Luo X. The synthesis and co-micellization of PCL-P (HEMA/HEMA-LA) and PCL-P (HEMA/HEMA-FA) as shell cross-linked drug carriers with target/redox properties. Journal of Biomaterials Science, Polymer Edition. 2019; 30(4): 276-294.
https://doi.org/10.1080/09205063.2018.1558486

15. Wu L, Mao G, Nian G, Xiang Y, Qian J, Qu S. Mechanical characterization and modeling of sponge-reinforced hydrogel composites under compression. Soft Matter. 2018; 14(21): 4355-4363.
https://doi.org/10.1039/C8SM00678D

16. Verma M, Biswal AK, Dhingra S, Gupta A, Saha S. Antibacterial response of polylactide surfaces modified with hydrophilic polymer brushes. Iranian Polymer Journal. 2019; 1-12.
https://doi.org/10.1007/s13726-019-00717-3

17. Jabbari S, Ghamkhari A, Javadzadeh Y, Salehi R, Davaran S. Doxorubicin and chrysin combination chemotherapy with novel pH-responsive poly [(lactide-co-glycolic acid)-block-methacrylic acid] nanoparticle. Journal of Drug Delivery Science and Technology. 2018; 46, 129-137.
https://doi.org/10.1016/j.jddst.2018.05.006

18. He Y, Yang Y, Ji X, Zhang Q, Jiang T, Shi H, et al. Preparation of polymer electrolyte membranes with continuous PEG channel via the fusion of self-assembled polycyclooctene-graft-polyethylene glycol copolymer micelles. Journal of Membrane Science. 2019; 572: 358-364.
https://doi.org/10.1016/j.memsci.2018.11.032

19. Pal A, Sarkar AN, Karmakar PD, Pal S. Amphiphilic graft copolymeric micelle using dextrin and poly (N-vinyl caprolactam) via RAFT polymerization: Development and application. International Journal of Biological Macromolecules. 2018; 119: 954-961.
https://doi.org/10.1016/j.ijbiomac.2018.07.198

20. Ghaleseiedi ZK, Tehrani AD, Parsamanesh M. Starch-based dual amphiphilic graft copolymer as a new pH-sensitive maltidrug co-delivery system. International Journal of Biological Macromolecules. 2018; 118: 913-920.
https://doi.org/10.1016/j.ijbiomac.2018.06.156

21. Lai GS, Lau WJ, Goh PS, Ismail AF, Tan YH, Chong CY, et al. Tailor-made thin film nanocomposite membrane incorporated with graphene oxide using novel interfacial polymerization technique for enhanced water separation. Chemical Engineering Journal. 2018; 344: 524-534.
https://doi.org/10.1016/j.cej.2018.03.116

22. Kazakova MA, Semikolenova NV, Korovin EY, Moseenkov SI, Andreev AS, Kachalov AS, et al. *In situ* polymerization technique for obtaining composite materials based on polyethylene, multi-walled carbon nanotubes and cobalt nanoparticles. Russian Journal of Applied Chemistry. 2018; 91(1): 127-135.
https://doi.org/10.1134/S1070427218010202

23. Iovu MC, Craley CR, Jeffries-El M, Krankowski AB, Zhang R, Kowalewski T, McCullough RD. Conducting regioregular polythiophene block copolymer nanofibrils synthesized by reversible addition fragmentation chain transfer polymerization (RAFT) and nitroxide mediated polymerization (NMP). Macromolecules. 2007; 40(14): 4733-4735.
https://doi.org/10.1021/ma070406x

24. Ribelli TG, Fantin M, Daran JC, Augustine KF, Poli R, Matyjaszewski K. Synthesis and characterization of the most active copper ATRP catalyst based on tris [(4-dimethylaminopyridyl) methyl] amine. Journal of the American Chemical Society. 2018; 140(4): 1525-1534.
https://doi.org/10.1021/jacs.7b12180

25. Ghamkhari A, Massoumi B, Jaymand M. Novel 'schizophrenic'diblock copolymer synthesized via RAFT polymerization: poly (2-succinyloxyethyl methacrylate)-b-poly [(N-4-vinyl-benzyl), N, N-

diethylamine]. Designed Monomers and Polymers. 2017; 20(1): 190-200. https://doi.org/10.1080/15685551.2016.1239165

26. Massoumi B, Mousavi-Hamamlu SV, Gham-khari A, Jaymand M. A novel strategy for synthesis of polystyrene/Fe3O4 nanocomposite: RAFT polymerization, functionalization, and coordination techniques. Polymer-Plastics Technology and Engineering. 2017; 56(8): 873-882. https://doi.org/10.1080/03602559.2016.1233270

27. Ghamkhari A, Pouyafar A, Salehi R, Rahbarghazi R. Chrysin and docetaxel loaded biodegradable micelle for combination chemotherapy of cancer stem cell. Pharmaceutical Research. 2019; 36(12): 165. https://doi.org/10.1007/s11095-019-2694-4

28. Ghamkhari A, Massoumi B, Salehi R. A new style for synthesis of thermo-responsive Fe3O4/poly (methylmethacrylate-b-N-isopropyl-acrylamide-b-acrylic acid) magnetic composite nanosphere and theranostic applications. Journal of Biomaterials science, Polymer edition. 2017; 28(17): 1985-2005. https://doi.org/10.1080/09205063.2017.1364459

29. Ghamkhari A, Agbolaghi S, Poorgholy N, Massoumi1 B. pH-responsive magnetic nanocomposites based on poly(2-succinyloxyethyl methacrylate-*co*-methylmethacrylate) for anticancer doxorubicin delivery applications. Journal of Polymer Research. 2018; 25(2): 37. https://doi.org/10.1007/s10965-017-1431-0

30. Ghamkhari A, Rahdar A, Rahdar S, Susan MABH. Dual responsive superparamagnetic nanocomposites: Synthesis, characterization and adsorption of nitrate from aqueous solution. Nano-Structures & Nano-Objects. 2019; 19:100371-100379. https://doi.org/10.1016/j.nanoso.2019.100371

31. Ghamkhari A, Ghorbani M, Aghbolaghi S. A perfect stimuli-responsive magnetic nano-composite for intracellular delivery of doxorubicin. Artificial Cells, Nanomedicine, and Biotechnology. 2018; 46(sup3): 911-921. https://doi.org/10.1080/21691401.2018.1518911